Supplementary Information

Energetics of water in the Solar System

Akshay K. Rao, Abhimanyu Das, Owen R Li, David M. Warsinger

Correspondence to: dwarsing@purdue.edu

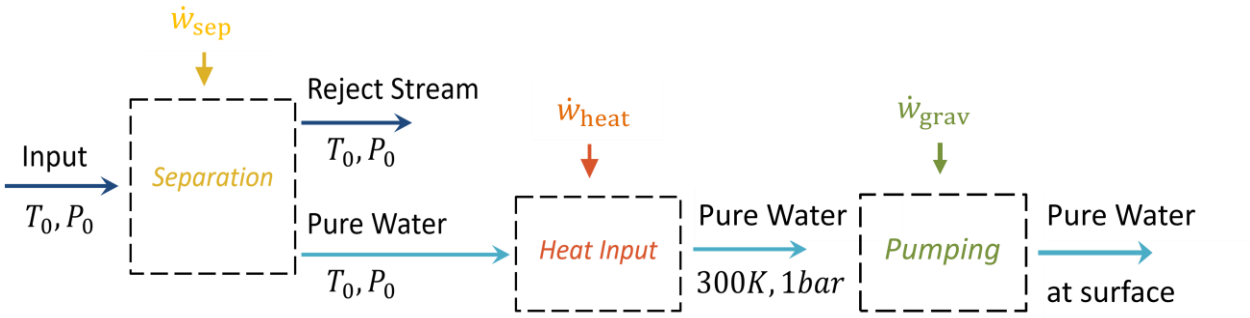

Fig. S1. Thermodynamic model visualization

The least work can be modeled as a staged, fully reversible process. The input and reject streams represent the feed and brine. These are evaluated the natural temperature of the source. The pure water from the input mixture is separated, isothermally using the minimum separation work described by S1. It is then brought to the Earth standard conditions, via the work due to heating. A third stage can be similarly added when gravitational potential is applicable.

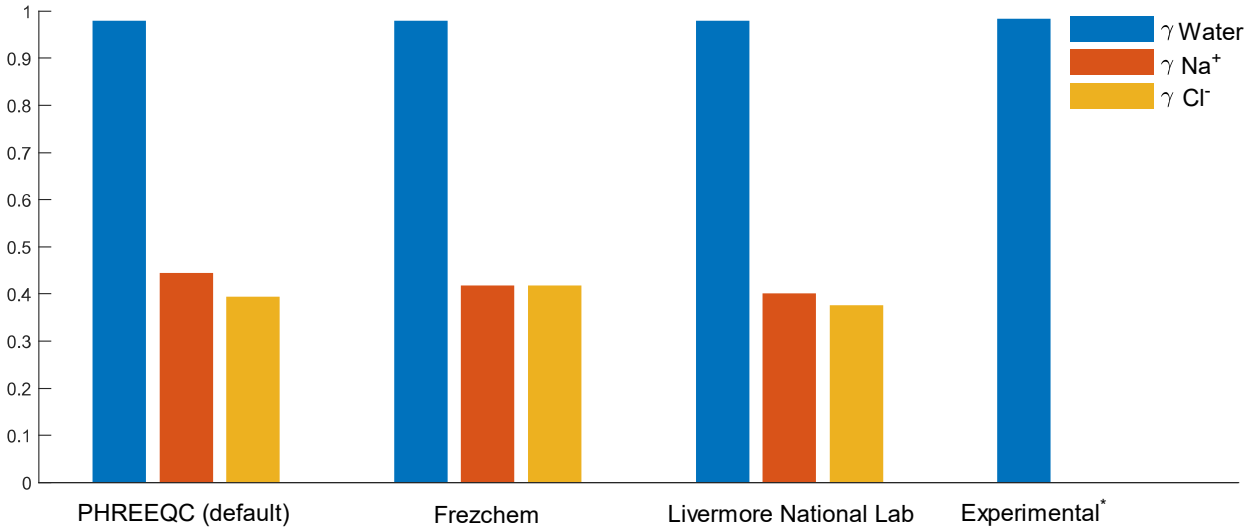

Fig. S2. PHREEQC model validation

A comparison of activity coefficient values to validate the thermochemical property models in PHREEQC is shown[1,2]. The activity of water, Na^+, and Cl^- are compared to prior literature for the thermochemical databases used in this study. The comparison was done at 300K and 0.596M (seawater salinity). The PHREEQC (default) and Livermore National Lab (LLNL) databases are publicly available at USGS. The Frezchem database is provided by Professor David Catling and Dr. Jon Toner [3–5]. Experimental values are provided at M = 0.6 from Chirife and Resnik (1984) [6].

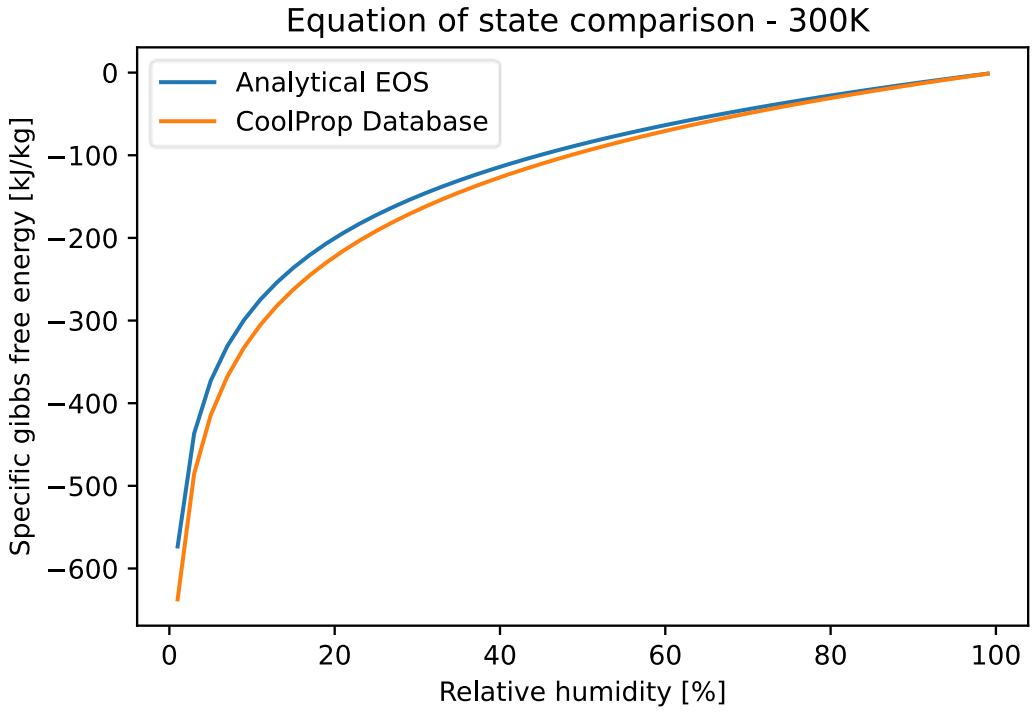

Fig. S3. Equation of state specific Gibbs free energy validation. The analytical EOS represents the property calculations based on the compressibility factor correlations, presented in methods. The CoolProp database of properties is validated against ASHRAE standards [7].

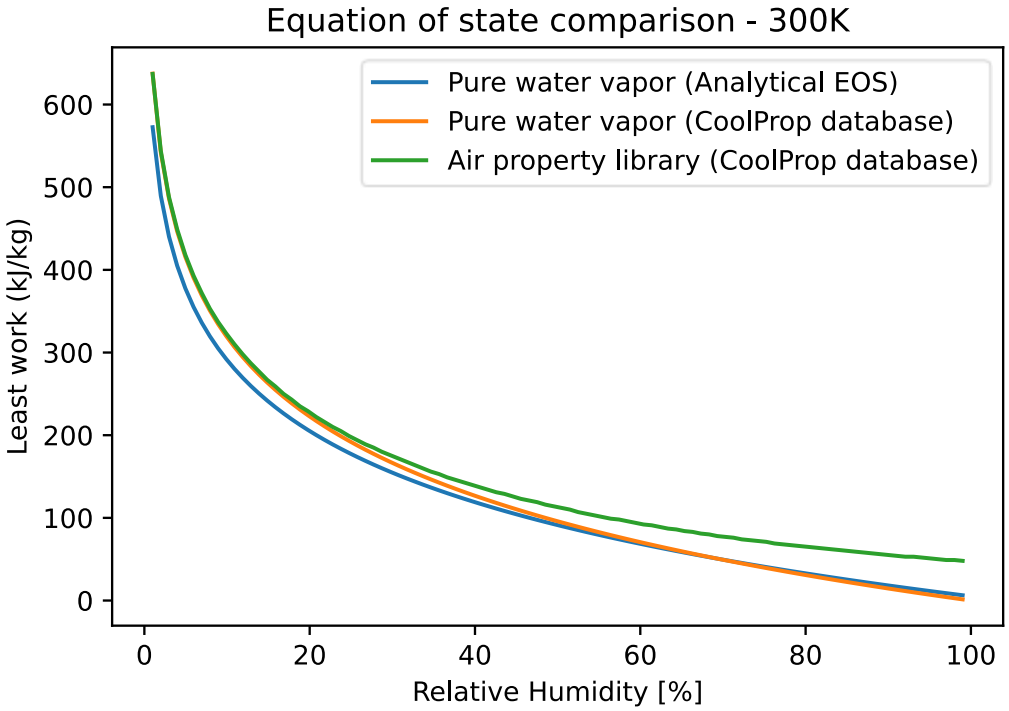

Fig. S4. Equation of state least work of separation validation. The calculation assumes an isothermal process at the thermodynamic dead state temperature (300K) to isolate the separation energy. The analytical equation of state (blue) and CoolProp property database (orange) are used for pure water vapor. The CoolProp database for humid air properties (green) is additionally used for comparison [7].

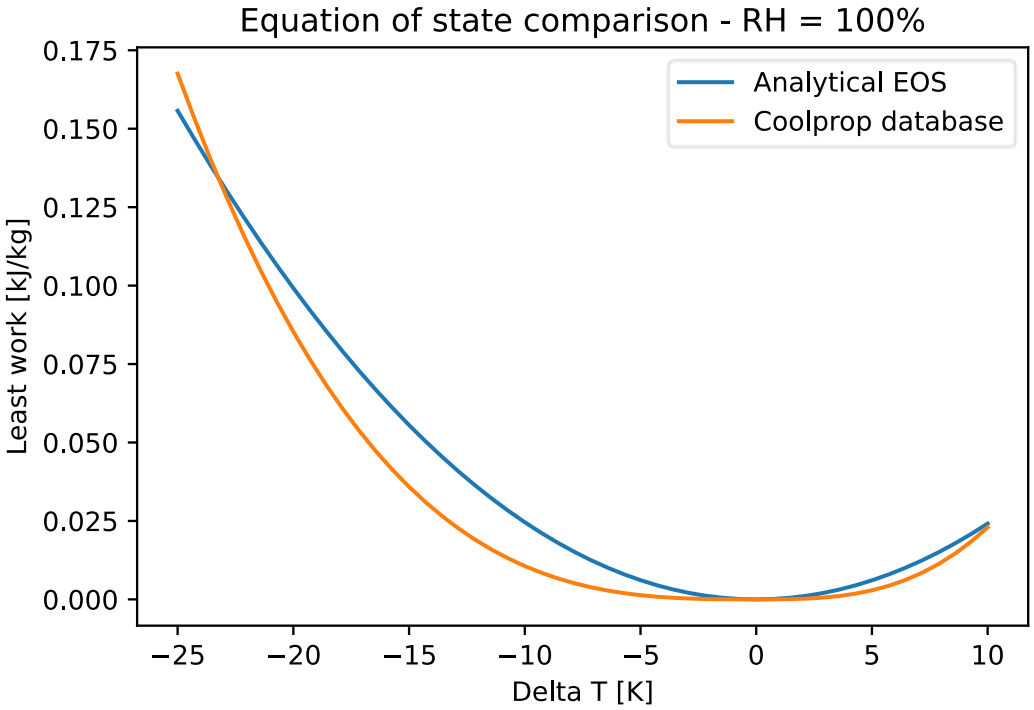

Fig. S5. Equation of state least work of heating validation. The calculation assumes an isobaric process at saturation (RH = 100%). The analytical equation of state (blue) and CoolProp database (orange) are used for pure water vapor [7]. Regardless of the equation of state, the least work approaches zero at the thermodynamic dead state.

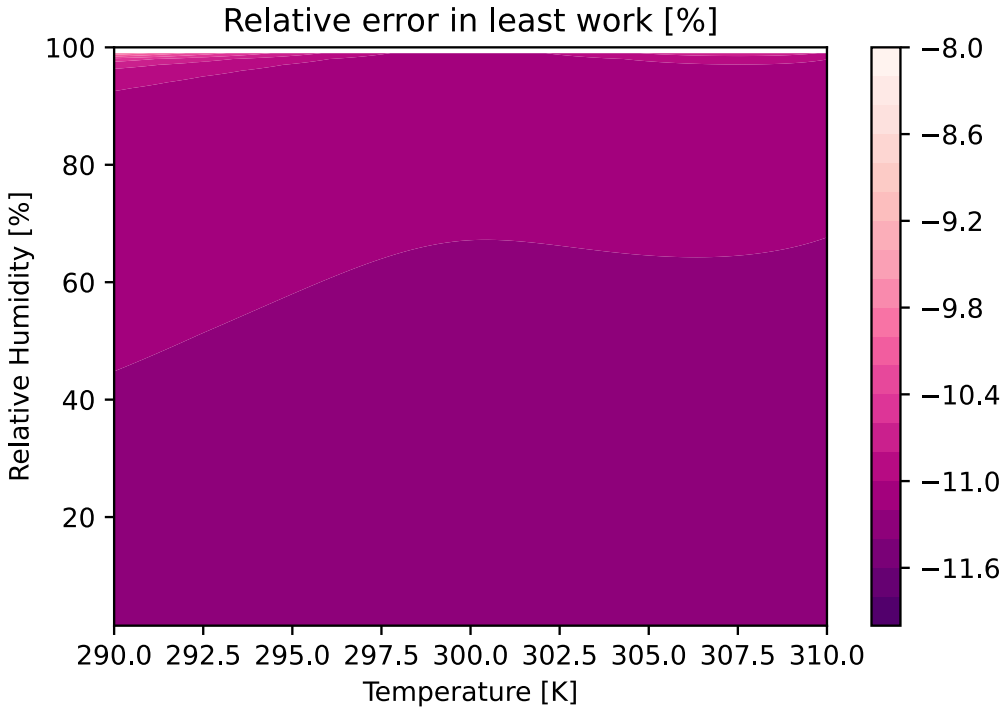

Fig. S6. Equation of state least work of heating validation. The calculation considers the total least work at ambient conditions that are well defined by the CoolProp database [7]. The relative error is calculated by $err = 100\left(\frac{W_{\text{analytical}} - W_{\text{CoolProp}}}{w_{\text{analytical}}}\right)$. The majority of the error may be attributed to the compressibility factor correlations since a 1st order Taylor series expansion in pressure was used. As shown by Wexler (1977) this error is reduced to less than 1% at temperatures below 273K [8], and therefore the range of this plot show the conditions of maximum model error.

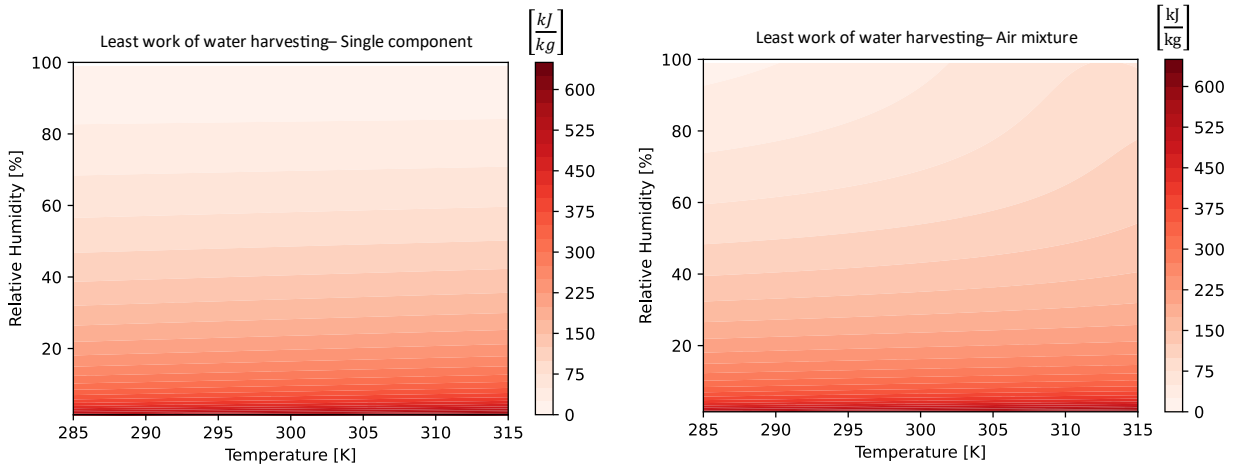

Fig. S7. Water harvesting from air and pure water vapor mixtures. This considers the full parametric sweep for water harvesting using the CoolProp database as the equation of state [7]. The single-component version (left) assumes Dalton's law and ignores other components in the mixture. The air version (right) assumes water is in a standard air mixture and accounts for energy interactions between mixture components. Nearly inert water vapor mixtures, like air, can behave as an ideal gas at low humidity. Water vapor on other planets is often found at low vapor pressures and concentrations. This suggests that the least work at low temperatures and humidity behaves similarly when computed with full mixture properties and water vapor partial properties.

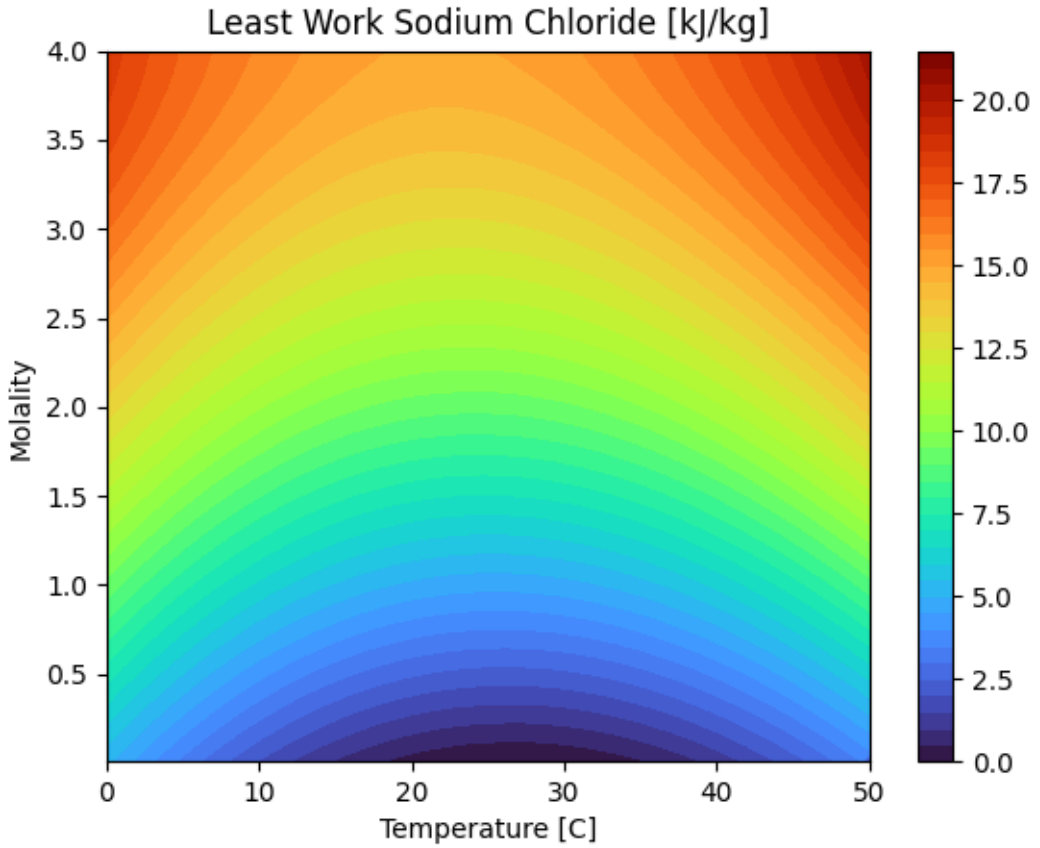

Fig. S8. Extended model of NaCl brine separation. Axes bounds represent the range of model validity. NaCl properties resemble water solutions on Earth and fall in between the upper and lower bounds shown in the manuscript Fig 1A. For reference, most solutions on Earth are less than 1m.

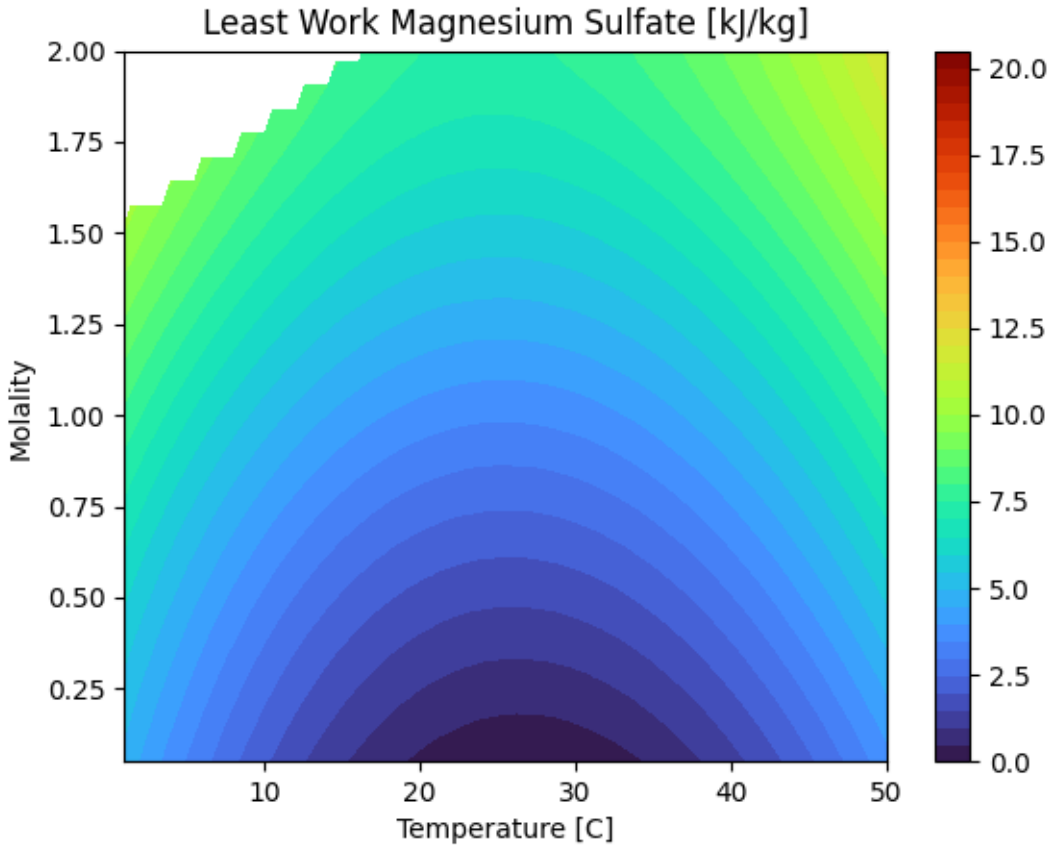

Fig. S9. Extended model for Mg (SO4)2 brine separation. Axes bounds represent the range of model validity. White space signifies supersaturation. Mg(SO4)2 solutions fall in between the upper and lower bounds shown in the manuscript Fig 1A.

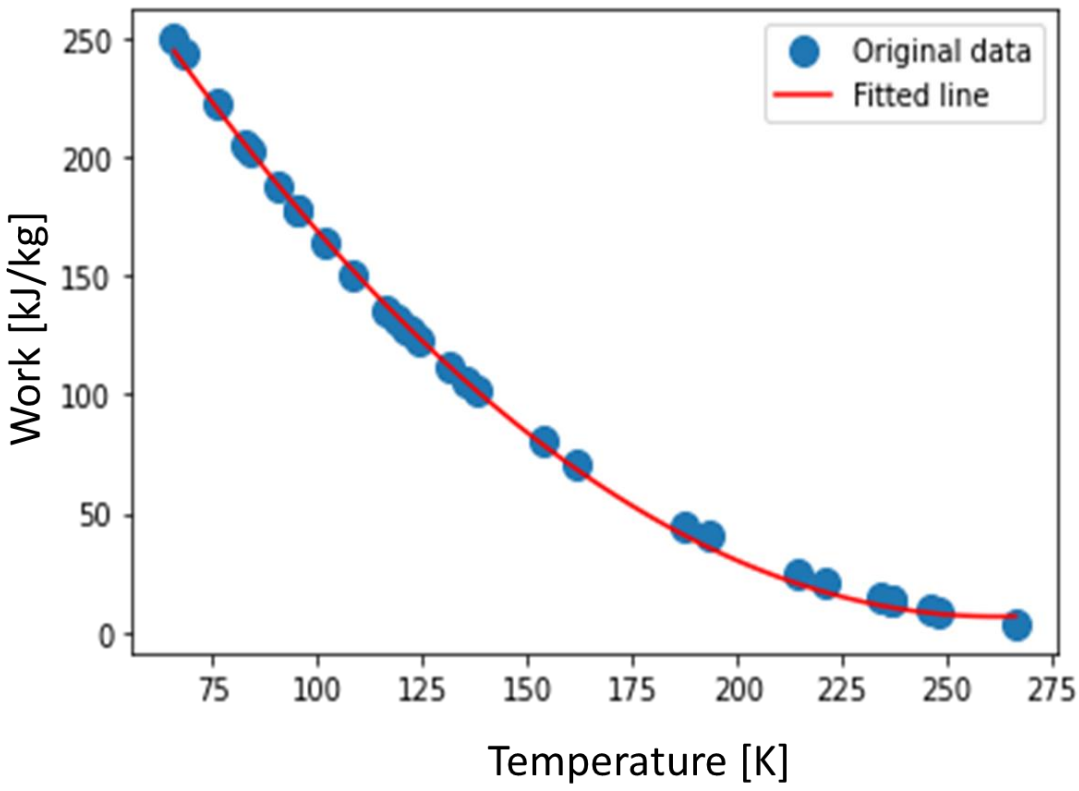

Fig. S10. Reduced order model for ice energetics. The least work (kJ/kg) model is fit to a 2nd degree polynomial on temperature (K): $W = 0.0062T^2 - 3.2436\ T\ +\ 430.8821$. Coefficients must be accurate to 4 decimal places. The original data refers to the calculations made for the manuscript Figure 2.

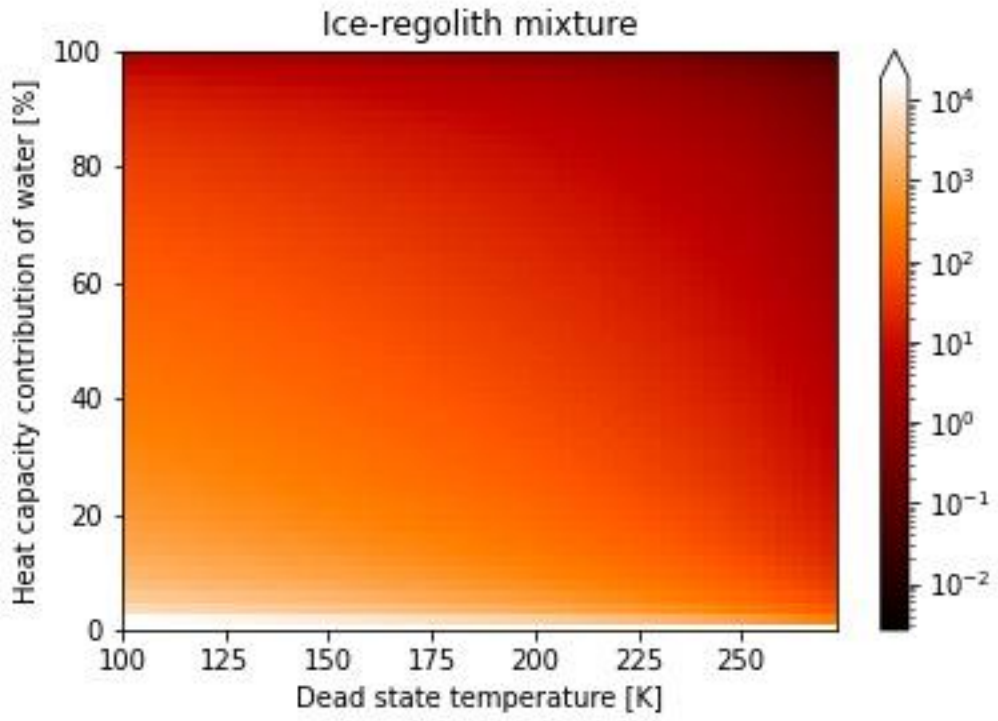

Fig. S11. Irreversibility of transient heating in physical mixtures like regolith. The heat capacity contribution of water encompasses the relative mass and specific heat capacity of water and the other species in the physical mixture. The energy is computed via the following equation:

$$\widetilde{W}_{\text{phys}} = \int_{T_0}^{300K} \left(1 - \frac{T_0}{T}\right) C_{\text{reg}} dT$$

Here, T_0 is the dead state temperature and C_{reg} is the constant pressure heat capacity of the non-water portion of the sample, on a per mass of water basis.

$$C_{\text{ratio}} = \frac{C_{\text{ice}}}{C_{\text{ice}} + C_{\text{reg}}} \rightarrow \frac{C_{\text{reg}}}{m_{\text{ice}}} = c_{\text{ice}} \left(\frac{1}{C_{\text{ratio}}} - 1\right)$$

The specific heat ratio, C_{ratio}, is shown on the y axis of the contour plot in S11 and represents the extensive heat capacity contribution of water-ice. Rearranging the equation for the heat capacity of regolith, C_{reg}, on a per mass of ice basis, m_{ice}, allows for a simple estimate in terms of just the specific heat capacity of ice, c_{ice}. This equation assumes the ratio of specific heats is constant through the heating process, with $c_{\text{ice}} = 2.108 \frac{\text{kJ}}{\text{kg K}}$. This is a reasonable assumption due to the incompressibility of solids within the shown temperature range.

Table S1. Water-Ice ranges of conditions. The explicit trials that are used for calculation can be found in Data S1.

Planetary Body	Temperature [K]	Depth [km]
Mercury	90 – 155	0
Earth	184 – 273	0
Moon	95 – 110	0
Mars	184 – 237	0
Europa	116 – 122	0
Ganymede	130 – 138	0
Enceladus	65 – 125	0
Tethys	75 – 85	0
Uranus	100 – 250	200-300
Jupiter	230 – 250	20-50

Table S2. Liquid water ranges of conditions. The explicit trials that are used for calculation can be found in Data S1.

Planetary Body	Temperature [K]	Depth [km]	Concentration [M]	Species Present
Earth	273 – 310	0	0.5 – 0.65	Na, Cl
Mars	271 – 285	0 – 0.75	0.4 – 1.2	Na, Mg, SO_4
Europa	272 – 325	10 – 30	0.9 – 1	Mg, SO_4
Ganymede	0 – 278	800	0.1 – 0.8	Na, Cl, HCO_3, CO_2, K
Enceladus	273 – 300	35	2.5 – 12	Na, Cl, Mg, K, Ca, ClO_4

Table S3. Water vapor ranges of conditions. The explicit trials that are used for calculation can be found in Data S1.

Planetary Body	Temperature [K]	Depth [km]	Vapor Pressure* [kPa]
Venus	430 – 740	0 – 50 **	0.006 – 0.5
Earth	273 – 325	0	0.2 - 13
Mars***	250 – 337	0	0.00005 – 0.0002

*Vapor pressure is used to represent mixing fraction and ambient pressure due to the ideal gas relationship

** The depth is considered for both accessing water at the mean planetary solid surface and the 1bar pressure level.

***Due to the extreme low pressures, water is able to stay in the vapor state at low temperatures.

Table S4. Brine solution comparison. All simulations, except for $\mathbf{ZnSO_4}$, use the FREZCHEM thermochemistry database provided by Professor David Catling. Since FREZCHEM does not include Zinc, it is simulated using the LLNL database. Each trial is simulated at 0.5 molality and 300 K. Trends are validated with prior literature on NaCl and $\mathbf{ZnSO_4}$ studies of least work and compared to the least work trends of five other relevant binary electrolyte solutions: KCl, $\mathbf{MgCl_2}$, $\mathbf{CaCl_2}$, $\mathbf{Na_2SO_4}$, and $\mathbf{MgSO_4}$. This comparison can be found in Figure 11 of Mistry, Hunter, Lienhard (2013) [9]**.**

Binary electrolyte solution	**Least work** $\left[\frac{kJ}{kg}\right]$
NaCl	2.42
$NaClO_4$	2.35
$Mg(ClO_4)_2$	4.02
$Ca(ClO_4)_2$	3.97
$ZnSO_4$	1.55

Table. S5. Compressibility factor validation. The calculation of the compressibility factor for sub-freezing temperatures is compared to the compressibility factor presented in Wexler (1997) [8]. The maximum percent difference between the two is 0.01%

	Compressibility factor Z [-]	
Temperature [K]	**This work**	**Wexler, 1977**
273.16	0.999624	0.999624
273.15	0.999624	0.999624
263.15	0.999807	0.999907
253.15	0.999907	0.999958
243.15	0.999959	0.999982
232.15	0.999982	0.999993
213.15	0.999999	0.99999
193.15	0.999999	1.00000
173.15	0.999999	1.00000

Data S1. (Separate file)

A component-wise breakdown of the results shown in Fig. 3 and the graphical abstract.

Additional References

1. Charlton, S. R. & Parkhurst, D. L. Modules based on the geochemical model PHREEQC for use in scripting and programming languages. *Computers and Geosciences* **37**, 1653–1663 (2011).

2. Parkhurst, D. & Appelo, C. *Description of Input and Examples for PHREEQC Version 3-A Computer Program for Speciation, Batch-Reaction, One-Dimensional Transport, and Inverse Geochemical Calculations*. http://www.hydrochemistry.eu.

3. Toner, J. D. & Catling, D. C. Water activities of NaClO4, Ca(ClO4)2, and Mg(ClO4)2 brines from experimental heat capacities: Water activity >0.6 below 200 K. *Geochimica et Cosmochimica Acta* **181**, 164–174 (2016).

4. Toner, J. D., Catling, D. C. & Light, B. The formation of supercooled brines, viscous liquids, and low-temperature perchlorate glasses in aqueous solutions relevant to Mars. *Icarus* **233**, 36–47 (2014).

5. Toner, J. D., Catling, D. C. & Light, B. Soluble salts at the Phoenix Lander site, Mars: A reanalysis of the Wet Chemistry Laboratory data. *Geochimica et Cosmochimica Acta* **136**, 142–168 (2014).

6. Chirife, J. & Resnik, S. L. Unsaturated Solutions of Sodium Chloride as Reference Sources of Water Activity at Various Temperatures. *Journal of Food Science* **49**, 1486–1488 (1984).

7. Bell, I. H., Wronski, J., Quoilin, S. & Lemort, V. Pure and pseudo-pure fluid thermophysical property evaluation and the open-source thermophysical property library coolprop. *Industrial and Engineering Chemistry Research* **53**, 2498–2508 (2014).

8. Wexler, A. VAPOR PRESSURE FORMULATION FOR ICE. *J Res Natl Bur Stand Sect A Phys Chem* **81 A**, 5–20 (1977).

9. Mistry, K. H., Hunter, H. A. & Lienhard V, J. H. Effect of composition and nonideal solution behavior on desalination calculations for mixed electrolyte solutions with comparison to seawater. *Desalination* **318**, 34–47 (2013).